# Determination of Thermal Simulation Performance with a Reduced-Scale Structure

**M.P. Modera**
*ASHRAE Associate Member*

ABSTRACT

The University of Liege has constructed a reduced-scale building model for use in determining and improving the accuracy of thermal simulation techniques. The model was designed to provide a high-precision data set that includes globe temperature, air temperature, internal and external surface temperatures, and laboratory and field climatological data. This report describes the construction and instrumentation of the model and the results of tests performed in the laboratory, including comparison with a finite-difference simulation of the dynamic tests.

Both the static and dynamic thermal characteristics of the model have been measured in the University of Liege wind-tunnel test chamber. The static heat losses were found to be very close to those determined by hand calculation, 5.44 to 5.54 Btu/hr°F (2.87-2.92 W/°C) in the laboratory, versus 5.42 Btu/hr°F (2.86 W/°C) by hand calculation. For the dynamic tests in the laboratory, as well as for the finite difference simulation of these tests, a two-time-constant fit was performed. For the response to a step increase in heat input, the laboratory measurements yielded time constants of 6.6 and 0.6 hours and the simulation predicted time constants of 5.9 and 0.8 hours.

The laboratory tests also provide insight into the importance certain heat-transfer phenomena will have in the field, such as the directional dependence of the external heat transfer coefficient and its effect on the thermal balance of the model.

## INTRODUCTION

A significant fraction of the building research under-way is concerned with the determination and the reduction of the energy required to provide human comfort. In most cases, the problem becomes one of predicting the future energy consumption of new or existing buildings. The conventional approach to this problem follows two parallel tracks: (1) using empirical data based upon laboratory and/or field measurements of the structure and its components; and (2) using mathematical simulations of the structure and its components, usually by computer. As a result of the obvious cost and time constraints associated with the first approach, the computer simulations have become the norm.

---

Work performed at Laboratoire de Physique du Batiment, University of Liege, Belgium.

Mark P. Modera Staff Scientist, Lawrence Berkeley Laboratory, Berkeley, CA.

Because computer simulations are used as research tools, design aids, audit bases, and a legal reference for building performance, questions about their accuracy and applicability quickly arise. An obvious solution to this problem is to compare computer predictions with situations for which measured data are available. This validation, which can be performed using either occupied or unoccupied structures, provides a measure of the total model performance and is usually sufficient for building simulations that average over reasonably long periods (eg., daily or weekly averages). A global validation of this sort is often unacceptable for research-oriented simulation models or any models designed to provide detailed (time steps of an hour or less) information about the evolution of indoor temperatures or heating system consumption. The margin of uncertainty associated with the measurements, as well as with the specification of the numerous physical parameters defining the structure, severely limits the generalization of the validation results.

To expand the applicability of validation work, the precision of the measurements must be improved, and the errors caused by the individual assumptions that form the basis of the model must be separated. An appropriate means for providing a detailed assessment of a model and its component parts is to choose an efficient form of problem reduction. A simple reduction of the size of the structure to be tested reduces uncertainties and makes the measurement of individual heat-transfer phenomena, such as the internal and external heat-transfer coefficients, more accessible.

The concept of a reduced-scale building model is not new to the research community.[1-3] The Centre Scientifique et Technique de la Construction (CSTC) has built and has conducted extensive field tests with a group of 12 one-cubic meter ($1m^3$) models.[4] The Laboratoire de Physique du Batiment (Building Physics Laboratory) at the Université de Liège has built a similar reduced-scale model that reduces experimental uncertainties even further using improved materials and measurement techniques.

This report describes the set of laboratory tests performed on the reduced scale structure built at Liege. These tests serve to improve the accuracy with which the static and dynamic thermal characteristics of the model can be specified. They also help determine the relative importance of the various measurements that can or will be made in the field.

## REDUCED-SCALE MODEL DESCRIPTION

As in any other case of problem reduction, it is necessary to determine which characteristics of the problem must be conserved. In the case of the reduced-scale model built at Liege, the concern is with testing the ability of computer simulations to track the evolution of the indoor temperature and/or heating load as a function of the solar input, outdoor temperature, and internal heat sources. In constructing a reduced-scale building model for this purpose, the relationships between the various heat-transfer mechanisms that determine the temperature within an full-scale structure should be maintained. For example, to conserve the basic nature of dynamic building response, the ratio of instantaneous heat losses to delayed heat losses (i.e., unshifted versus phase-shifted heat losses) must be preserved. The ratio of glazing to opaque surface area is also important because it controls the relationship between the effects of transmitted sunlight and that absorbed by opaque surfaces. This ratio also the determines the extent to which the external heat-transfer coefficient affects the thermal response of the building. The relationships above differentiate the problem of modeling a building from that of modeling a wall. Because the effect of the sun and its dependence on the condition of the sky are important to our research program, the model must be placed in the actual terrain, eliminating the possibility of using exotic gases in a laboratory wind tunnel.

## General Construction

The model is a 1-$m^3$ box with a single double-pane window (see Fig. 1). The basic structure consists of an aluminum cube insulated on both sides with polyurethane boards and protected externally with plasticized plywood. The windowed wall is removable and can be replaced by a windowless panel. This feature provides access to the interior of the model, and allows for tests both with and without the window. The floor of the model is covered with a removable aluminum plate to provide internal thermal mass and the resultant phase shift between solar inputs and indoor (globe) temperature response.

## Thermal Characteristics

The walls of the model were designed to provide a clear distinction between resistance and thermal capacity. This design makes the model suitable for analysis with lumped-parameter wall representations as well as with the more complex representations typical of large computer simulations. The location of the majority of thermal mass is known precisely, and the wall can be represented by a simple RC circuit, Fig. 2. The aluminum cube, indicated by $C_a$, represents 41% of the total thermal capacity. The wooden shell provides 45% of the capacity, leaving only 14% of the capacity to be distributed within the resistive elements. Similarly, about 90% of the thermal resistance of the wall is in the insulation layers. This allows measurement of the evolution of the thermal mass temperatures as a function of internal or external heat fluxes or temperature changes.

The heat loss resulting from air infiltration is provided by four identical apertures at the same height in each of the model walls. Because the walls of the welded aluminum box are airtight, this system prevents stack-induced air infiltration, the resulting infiltration rate depending only on wind speed and direction. The infiltration holes were scaled to provide 25 to 30% of the total heat loss of the model, as is typical in residential dwellings.

In the field, the infiltration rate will be measured using a tracer gas technique. Correlation of these infiltration measurements with wind speed and direction will also be attempted.

## Model Instrumentation

A basic interest in the reduced-scale model is to examine our ability to track the globe temperature of a building. To this end, the model is fitted with a 4 in. (10 cm) diameter globe temperature sensor (black), placed to eliminate the possibility of direct solar insolation. To further define the thermal performance of the model, it is also fitted with a variety of supplementary sensors, including at least one for measuring indoor air temperature.

The interior climate is more precisely defined by surface temperature measurements of the floor, ceiling, walls, and aluminum floor plate. The surface temperatures are measured with four 4 in. (10 cm) square copper plates on each wall, distributed such that each plate represents one quarter of the surface area of the wall. These indoor surface temperatures also represent one side of the integral heat flux meter formed by the (0. 8 in. [2 cm] thick) internal insulation panels. In total, there are four measurements for each wall of the model: the internal surface temperature, the temperature at the internal insulation-aluminum interface, the temperature drop across the internal insulation, and the temperature at the insulation-wood interface (see Fig. 3).

This measurement network allows for detailed analysis of the conductive heat losses of the model, providing a picture of the energy flows within the walls. Measurements of the heat flux through each wall provide an additional check on the thermal balance of the model and can be combined with the internal surface temperatures and the wooden shell temperatures to approximate the internal and external heat transfer coefficients. Although the accuracy of the heat-flux measurement is limited by the thermal capacity of the insulation, the time constant of the panel is sufficiently small to ensure the usefulness of the measurement. In addition, the internal and external temperatures of the window are measured, providing reasonable estimates of the heat flux and heat transfer coefficients during periods without sunlight.

All of the temperature measurements are made with Type T (copper- constantan) thermocouples. The couples are all made from the same spool of wire, ensuring that an average calibration will be sufficient. (Direct voltage measurements are converted to temperatures with a three-parameter calibration of 10 sample couples.)

The model is fitted with three separate heating systems: (1) a conventional free-convection/radiative unit installed below the window, (2) a forced convection unit, and (3) a radiative/convective system incorporated into the floor of the model. The three systems provide a base for testing the short-term response to different types of internal heat sources. The window unit approximates realistic heating conditions, whereas the forced convection unit simulates the conventional assumption of perfectly mixed indoor air. The third heating system will act as a "thermally heavy" unit because of the high thermal mass of the aluminum floor plate. The globe temperature measurement will be used as the control signal for all heating systems, eliminating discrepancies between the control signal and the temperature to be controlled.

### Data Acquisition

The reduced-scale model is accompanied by a central data-acquisition system for laboratory and on-site tests. With this system, measurements are taken every 30 s, and stored as 10-min averages with standard deviations. This form of storage filters high-frequency noise from the data and has the additional advantage of acting as an integrator for solar insolation measurements, thus reducing measurement uncertainties.

## STATIC THERMAL PARAMETERS: LABORATORY TESTS

The full set of laboratory tests of the reduced-scale model were performed in the wind-tunnel test chamber represented in Fig. 4. The chamber is cooled with a thermostated refrigerant loop that can maintain the air temperature as low as 32°F (0°C). Air mixing and wind simulation are provided by four large blowers which allow adjustment of the windspeed between approximately 3 ft/s (1 m/s) and 13 ft/s (4 m/s). The wind profile does not approximate the boundary layer flow found in the field but can be used to examine the effects of wind speed and direction on the thermal balance of the model.

### Definition of the Climate Within the Chamber

The determination of the overall thermal conductance (UA value), the model's single most important thermal parameter, requires a precise definition of the internal and external climates. Internal climate is characterized by the resultant (or globe) temperature. Similarly, the characterization of external climate must consider both radiative and convective exchanges. Because the convective and radiative heat transfer coefficients are similar in

magnitude, the chamber climate is defined by the average of the air temperature and the mean radiant temperature. The mean radiant temperature is determined using the surface temperatures measured on all of the chamber walls. Figure 5 is a plot of the air temperature, mean radiant temperature, and resultant chamber temperature for a typical test period.

## Overall Thermal Conductance

The overall thermal conductance of the model has been measured for seven test periods that were designed to separate the different phenomena affecting the thermal balance of the model. To examine the effect of external convection coefficients as a function of wind direction, the rotation of the model was changed to alter the angle of attack of the wind. Tests were also made with and without air infiltration, with and without the window, and with the three types of heating systems. A summary of these tests is in Tab. 1.

The calculated conductances in Tab. 1 were determined using handbook conductivities and account for the bidimensional characteristics of the walls. The heat loss resulting from infiltration was calculated using the Lawrence Berkeley Laboratory predictive infiltration model.[5] The predicted infiltration rate is proportional to the model's leakage area, which was measured using the fan pressurization technique.

## External Heat Transfer Coefficients

The calculated conductances (UA values) correspond well with the measured values, although the calculated values do not account for variations with wind direction. By rotating the model window relative to the incoming wind, the importance of wind direction can be seen. In Tab. 1, a wind direction of $0^{o}$ corresponds to flow perpendicular to the window, and an angle of $90^{o}$ corresponds to wind parallel to the surface of the window. Because the external heat-transfer coefficient of the window represents as much as a third of its thermal resistance, the angle of attack on the window has a measurable effect on the heat loss of the model (tests 3, 4, and 5). Figures 6 and 7 display the importance of this effect quite dramatically. Figure 6 is a plot of the external surface temperature of the window, and Fig. 7 is a plot of the internal temperature of the window during the course of the model rotations. The first section of each plot represents the period during which the wind hits the window perpendicularly, followed by flow parallel to the window surface, and finally, flow at $45^{o}$ to the surface of the window. Subtracting the external surface temperature from the internal surface temperature during each period yields temperature differences of 29.3 $F^{o}$ (16.3$^{o}$C), 27.0 $F^{o}$ (15.0$^{o}$C), and 28.1 $F^{o}$ (15.6$^{o}$C), corresponding to heat losses of 137 Btu/h (40.2 W), 126 Btu/h (37.0 W), and 131 Btu/h (38.5 W). In this case, the error caused by ignoring the directional variation of the convective heat-transfer coefficient of the window represents 3% of the total heat loss of the model. This test demonstrates an often ignored source of error, especially important in the case of a high-precision model validation.

To further examine the sensitivity of the external heat transfer coefficient, this parameter was calculated for each of the model walls, using heat fluxes measured with the integral heat flux meters. In each case, the convective component of the heat transfer coefficient was isolated from the radiative component. The convective heat-transfer coefficients for the four walls and the window are presented in Tab. 2. This table demonstrates the dependence of these coefficients on the wind speed and wind direction. The directional effects are especially evident for the model window.

Comparing the convective heat transfer coefficients of the window for tests 3 and 4 reveals a 40% decrease for airflow parallel to the window surface (test 4), relative to perpendicular flow (test 3). Test 5, which represents wind at a 45° angle of attack, indicates that the coefficient may vary linearly with the wind direction. This result is clearly reproduced on the south wall, although the east wall does not exhibit this effect. In test 5, the northern and western walls are placed symmetrically on the downwind side at 45° angles to the wind. The convective coefficients are essentially equal, as expected, and exhibit similar tendencies when the walls are switched between the downwind position and a position parallel to the wind (tests 3 and 4). These variations can be quite important, because the internal temperature response to insolation on opaque surfaces is directly proportional to the external heat-transfer coefficients. Because the wind speed and wind direction are not well-correlated with solar heat fluxes on a given surface, the effect in question is also non-linear. The heat-transfer coefficient is especially important in the case of the reduced-scale model because the absorbed solar energy represents a large fraction of the total temperature response.

## Heat Flux Measurements

To check the accuracy of the heat flux sensors incorporated into the internal insulation panels, measured heat fluxes are compared with total power injected into the model by the heating system. The results of these comparisons for the first five static tests are presented in Tab. 3.

The results in Tab. 3 are quite encouraging, indicating that the heat flux sensors can be used to measure the heat loss of the model, at least under steady-state conditions. For the test without the window (test 1), the measured fluxes are approximately equal in all walls -- slightly higher at the roof, and slightly lower on the floor, as expected. The total-heat-loss calculation also appears to be accurate, even in the tests that include the model window (whose heat flux accuracy might be questioned). The discrepancies that do exist, -7.3% for test 1 and +4.8% for test 2, could be explained by the temperature dependence of the internal insulation conductivity, to which the calculated heat fluxes are directly proportional. The conductivity increases with temperature, implying that heat fluxes will be underestimated at high temperatures and overestimated at low temperatures, corresponding to the observed results.

## DYNAMIC THERMAL PARAMETERS: LABORATORY TESTS

The laboratory test chamber is well-suited for determining the dynamic thermal characteristics of the model. Although the chamber temperature exhibits a small diurnal swing, the overall climate is much more easily defined and controlled than that in the field.

The dynamic tests performed within the chamber consisted of maintaining a constant chamber temperature and submitting the model to a step change of internal heating power. The time constant associated with these types of tests is about three times as long as that associated with heating consumption response to external temperature changes. Despite this disadvantage, the temperature-response tests are much easier to perform, because the thermal capacity of the test chamber makes it difficult to produce the temperature profiles required for heating-consumption-response tests.

As a means of quantifying the results of the dynamic tests, the temperature response profiles were fitted to a two-time-constant, three-parameter

exponential (Eq.1), using the Gauss-Newton least-squares technique.

$$T = T_f \left(1 - [1 - \theta]\, e^{\frac{-t}{\tau_1}} - \theta\, e^{\frac{-t}{\tau_2}}\right) \qquad (1)$$

where

- $T$ resultant temperature of the model, $^oF$ ($^oC$)
- $T_f$ resultant temperature at steady-state conditions, $^oF$ ($^oC$)
- $\tau_1$ long time constant of the model, h
- $\tau_2$ short time constant of the model, h
- $\theta$ parameter describing the relative importance of the two time constants (dimensionless)

It has been shown that a simplified model of this sort provides a reasonable estimate of building response over a sufficiently large frequency range.[6,7] Table 4 provides a summary of the analyses of four step response tests in the laboratory.

The results of the dynamic tests presented in Tab. 4 are quite consistent, pinning the most important dynamic parameter, the long time constant, down to about 6 1/2 hours. The amplitude reduction and phase lag of external temperature changes or solar heat fluxes are basically determined by this time constant. The parameter $\theta$ is also quite well-determined, the short time constant of the model being the only parameter that appears to be uncertain. This parameter is normally more difficult to determine, yet the discrepancies appear only in the two tests that include air infiltration.

Certain results that might be helpful do not appear in Tab. 4, e.g., a difference in the short time constant of the model resulting from two different types of heating systems, or the addition of air infiltration. The short time constant is associated with the thermal capacity of the room air, although a calculation using just this capacity yields much too short a time constant when compared with experimental results. One explanation for this is that the room air requires time to mix and achieve its steady state temperature distribution, thereby introducing an additional time lag into the system.

A comparsion of a well-mixed situation (test A with fan) with the usual free-convection situation (test B) was made. Unfortunately, the expected difference due to the lack of mixing fan in test B is not seen. This may suggest that the effect of air mixing may be minimized by the size and shape of the reduced scale model. Another possible explanation is that a large fraction of the actual time lag may be attributed to the internal aluminum plate. The temperature of the aluminum plate may be more closely coupled to the globe temperature than to the temperature of the thermal mass in the walls. In a real structure the latter explanation applies to the mass of internal furnishings, and could be extended to include a thin layer of the internal walls. A thin surface layer is more closely tied to the internal air temperature than to the thermal mass of the wall.

## FINITE-DIFFERENCE SIMULATION

As a start on the validation work to be performed with the reduced-scale model, a simulation of the model response to a step increase in heating power was performed using a finite difference program, LPB-1.[8] In this simulation, the overall conductance of the model was assumed to be 5.54 Btu/hr$^o$F, (2.92 W/$^o$C), consistent with the values measured in the laboratory test chamber. In the simulation, the model was subjected to a step increase in heating power from 0 to 164 Btu/hr, (0 W to 48 W). The resulting temperature response curve

was then fitted using Eq. 1, yielding values of 5.9 h for the long time constant, 0.79 h for the short time constant, and 0.13 for $\Theta$. When compared with the results obtained for the laboratory tests, the long time constant appears to be about 10% low, the short time constant about 40% high, and $\Theta$ about half its laboratory value. Although the long time constant prediction is acceptable, a greater accuracy would be expected. The discrepancies in the short time constant, and in $\Theta$, are not troublesome, since the thermal capacity of the room air was severely augmented in the simulation, as is the practice in full-scale structures when using the LPB-1 program. Reducing the capacity towards its actual value decreases the short time constant, and the long time constant should move toward its measured value.

## CONCLUSIONS

This report has described the reduced-scale model project currently under way at the University of Liege, including a description of the model and a short description of the laboratory tests performed before the model was installed for field measurements. The laboratory tests have provided well-determined values for both the static and dynamic thermal characteristics of the model. Fixing these parameters in the laboratory limits the number of free parameters available during the analysis of field data, thereby reducing the uncertainties in the analysis. The laboratory tests have also provided confidence in the measurement apparatus, including the integral heat flux sensors, which provided accurate and consistent results.

The long-term goal of this project was to build a basic research tool for examining the thermal behavior of buildings,as well as to provide a reliable data base with which the multiple computer simulations can be compared. The laboratory tests described herein have provided some insight into the subtleties of making thermal predictions often overlooked or too complex to account for in full-scale building measurements. For example, the external convection coefficient varies considerably with wind direction and can have an important effect on the thermal balance of the model.

## REFERENCES


1. J. Lebrun and H. Heikhaus, "The Temperature Without Heating of a Building and Heating Energy Consumption: Experimental Steady State Analysis on Reduced Scale Models," Proceedings of the International Energy Agency Conference. (Berlin: April 1981.)

2. R.W. Richardson and S.M., Berman, Dynamic Similitude in Scale Models of Buildings. (Lawrence Berkeley Laboratory report [LBL-13262] , 1981.)

3. B. Andersson, F. Bauman, and R. Kammerud, Verification of BLAST by Comparison with Direct Gain Test Cell Measurements (Lawrence Berkeley Laboratory report [LBL-10619] , 1980.)

4. H. Heikhaus and J. Lebrun, "Thermal Monitoring of a Dozen Reduced Scale Models of Houses" (Paper delivered at Symposium organized by the C.E.C., DGXII-C Energy Research Program, Comparative Experimentation of Low-Energy Houses, Liege, May 1981).

5. M.H. Sherman and D.T. Grimsrud, Measurement of Infiltration Using Fan Pressurization and Weather Data (Lawrence Berkeley Laboratory report [LBL-10852] , 1980.)

6. L. Laret, "Contribution aux developpements de modeles mathematiques du comportement transitoire de structures d'habitationsi," These de doctorat

en Sciences Appliquees (Universite de Liege, Laboratoire de Physique du Batiment. May 1980).

7. L. Laret, Some Comments on Concept of Simplified Dynamic Modelling of Building Thermal Behavior (University of Liege, Laboratoire de Physique du Batiment [LL82041501]).

8. Y. Delorme, L. Laret, and H. Sohet, "Numerical Predictions of Thermal Behavior in Dwelling Structures" (Paper presented at Collection des Publications de la Faculte des Sciences Appliquees de L'Universite de Liege n° 83 de 1980).

TABLE 1
Overall Thermal Conductance Tests

| | Test Number | | | | | | |
|---|---|---|---|---|---|---|---|
| | 1 | 2 | 3 | 4 | 5 | 6 | 7 |
| UA(calculated), Btu/hr°F (w/°C) | 3.96 (2.09) | 5.42 (2.86) | 5.42 (2.86) | 5.42 (2.86) | 5.42 (2.86) | 5.95 (3.14) | 5.95 (3.14) |
| UA(measured), Btu/hr°F (W/°C) | 3.79 (2.00) | 5.54 (2.92) | 5.54 (2.92) | 5.44 (2.87) | 5.50 (2.90) | 5.84 (3.08) | 5.76 (3.04) |
| Window | No | Yes | Yes | Yes | Yes | Yes | Yes |
| Window orientation Deg. | N/A | 0 | 0 | 90 | 45 | 0 | 0 |
| Windspeed, Ft/s (m/s) | 13 (4) | 3 (1) | 3 (1) | 3 (1) | 3 (1) | 3 (1) | 3 (1) |
| Infiltration | No | No | No | No | No | Yes | Yes |
| Heating system | Fan | Fan | Nat Conv | Nat Conv | Nat Conv | Rad | Nat Conv |
| Number of 10-min. periods | 100 | 49 | 99 | 100 | 28 | 20 | 20 |

TABLE 2

Convective Component of External Heat Transfer Coefficient.*

| Wall∀ | Test Number | | | | |
|---|---|---|---|---|---|
| | 1 | 2 | 3 | 4 | 5 |
| Window | N/A | 1.82 (10.3) | 1.69 (9.6) | 1.00 (5.7) | 1.32 (7.5) |
| South | 1.07 (6.1) | 0.32 (1.8) | 0.41 (2.3) | 0.26 (1.5) | 0.32 (1.8) |
| North | 0.79 (4.5) | 0.09 (0.5) | 0.14 (0.8) | 0.42 (2.4) | 0.37 (2.1) |
| East | 0.85 (4.8) | 0.48 (2.7) | 0.44 (2.5) | 0.44 (2.5) | 0.44 (2.5) |
| West | 0.74 (4.2) | 0.26 (1.5) | 0.26 (1.5) | 0.19 (1.1) | 0.35 (2.0) |

* All values in units of BTU/hr $ft^2$ $^oF$, ($W/m^2$ $^oC$).

∀ In the field, the windowed wall will face south.

TABLE 3

Comparison of Measured Heat Fluxes With Heater Consumption*

| Surface | Test number | | | | |
|---|---|---|---|---|---|
| | 1 | 2 | 3 | 4 | 5 |
| Roof | 54.3 (15.9) | 18.1 (5.3) | 36.2 (10.6) | 37.2 (10.9) | 36.2 (10.6) |
| North | 52.2 (15.3) | 17.1 (5.0) | 33.8 (9.9) | 34.5 (10.1) | 33.8 (9.9) |
| East | 53.3 (15.6) | 17.4 (5.1) | 36.5 (10.7) | 37.2 (10.9) | 36.5 (10.7) |
| West | 52.6 (15.4) | 17.4 (5.1) | 35.5 (10.4) | 36.2 (10.6) | 35.5 (10.4) |
| South | 52.9 (15.5) | 12.3 (3.6) | 24.6 (7.2) | 24.9 (7.3) | 24.2 (7.1) |
| Floor | 51.2 (15.0) | 17.1 (5.0) | 34.5 (10.1) | 34.8 (10.2) | 34.1 (10.0) |
| Window | N/A | 69.0 (20.2) | 132 (38.8) | 122 (35.7) | 128 (37.4) |
| Total | 317 (92.7) | 168 (49.4) | 334 (97.8) | 327 (95.8) | 328 (96.1) |
| Heater Power | 341 (100) | 160 (47) | 331 (97) | 331 (97) | 332 (97) |
| Error | -7.3% | 4.8% | 0.8% | -1.2% | -0.9% |

* All fluxes in Btu/hr (Watts).

TABLE 4

Double Exponential Fits of Dynamic Tests

| Dynamic Test | Initial Heating Power Btu/h (W) | Final Heating Power Btu/h (W) | Heating System | Air Infiltration | $t_1$ (hr) | $t_2$ (hr) | Q |
|---|---|---|---|---|---|---|---|
| A | 160 (47) | 335 (98) | Fan | No | 6.8 | 0.58 | 0.29 |
| B | 331 (97) | 174 (51) | Nat | No | 6.5 | 0.58 | 0.27 |
| C | 0 (0) | 341 (100) | Nat | Yes | 6.5 | 0.33 | 0.29 |
| D | 174 (51) | 0 (0) | Nat | Yes | 6.7 | 0.72 | 0.29 |

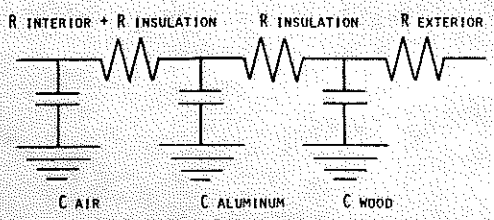


*Figure 2. Electrical analog of model walls*

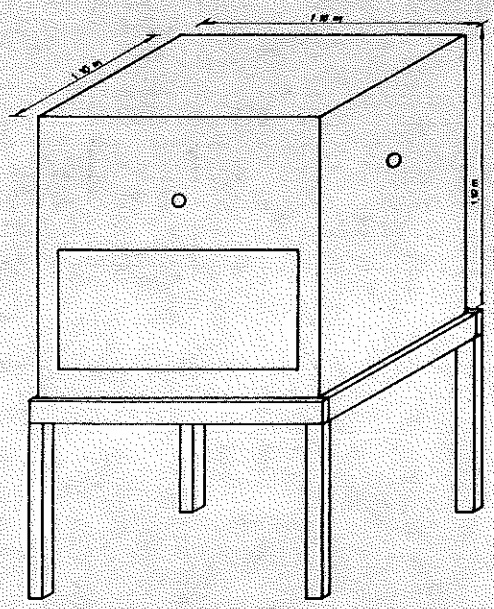

*Figure 1. Reduced-scale model as it will be installed in the field*

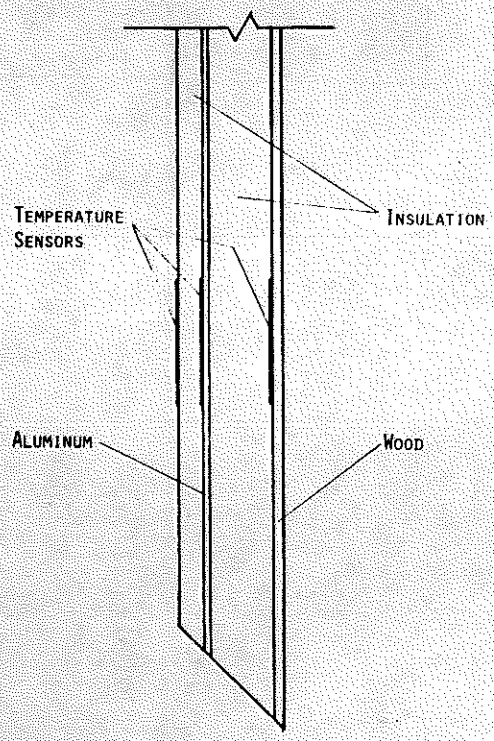


*Figure 3. Cross section of a model wall*

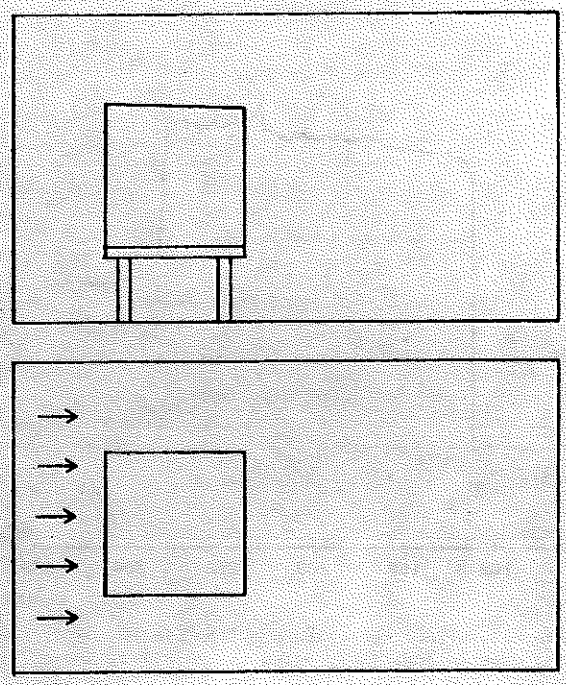

*Figure 4. Model within the wind tunnel test chamber*

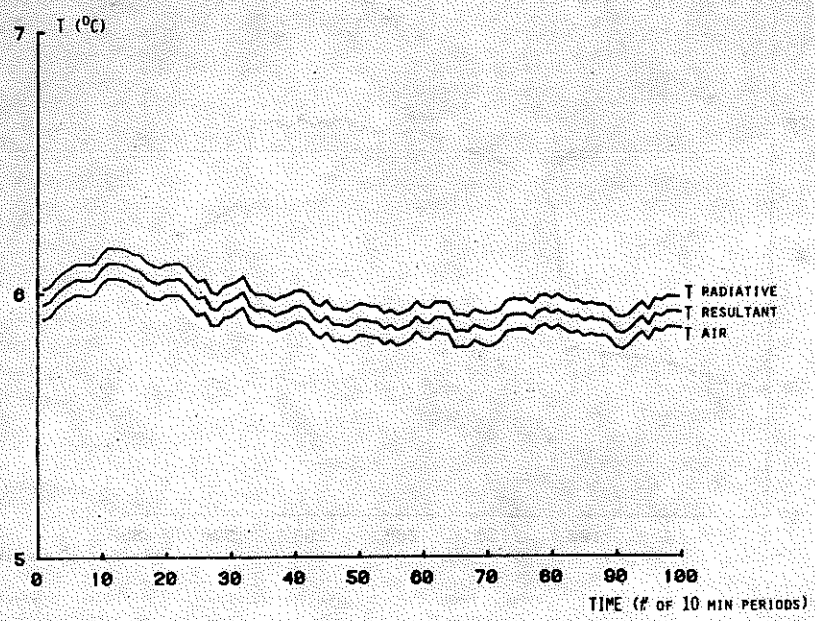


*Figure 5. Radiant temperature, air temperature, and resultant temperature within the test chamber*

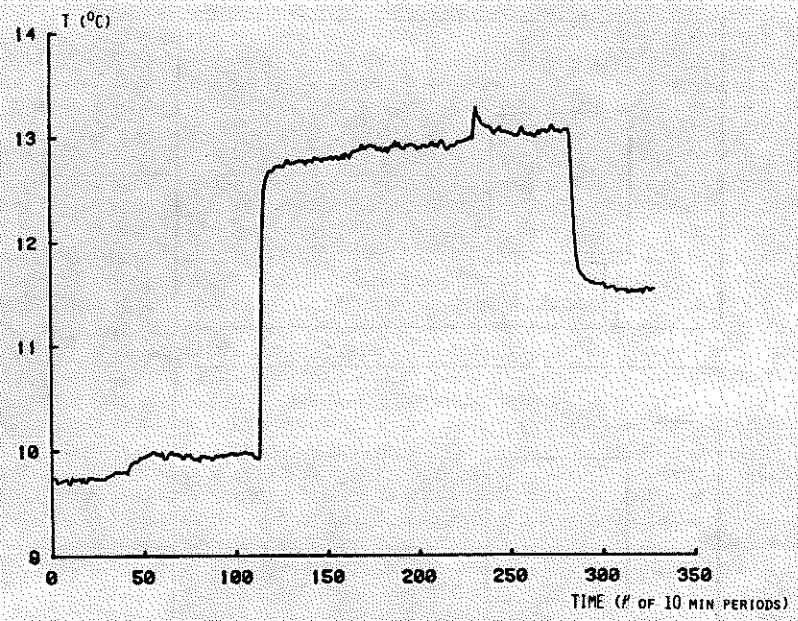


*Figure 6.* *External surface temperature of the window for different wind orientations (perpendicular, parallel, and 45° to window)*

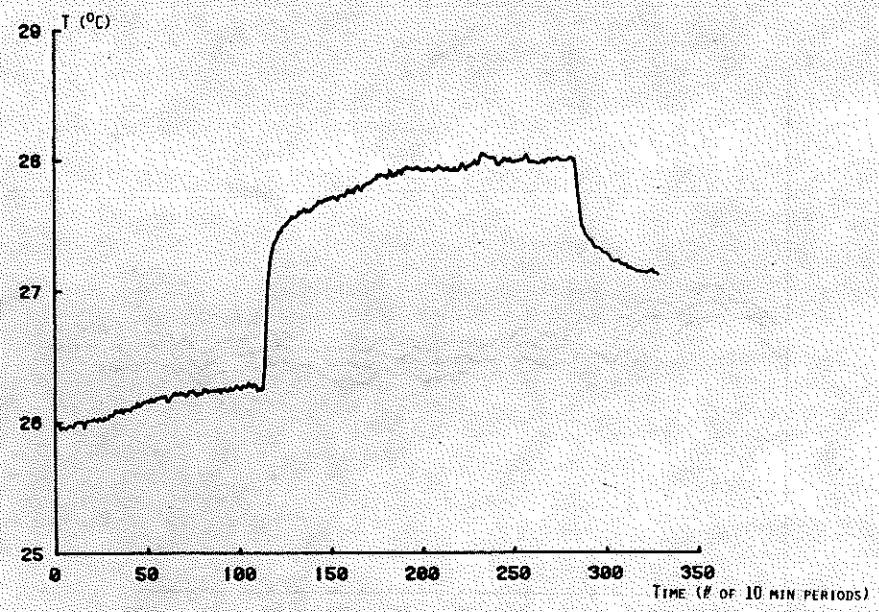


*Figure 7.* *Internal surface temperature of the window for different wind orientations (perpendicular, parallel, and 45° to window)*

# Discussion

M. Masoero, Politecnico di Torino, Torino, Italy: Can you explain how the surface temperature of the windows was measured?

M. Modera: The surface temperatures of the windows are measured with thermocouples on 1 cm diameter copper disks. The accuracy of these measurements is expected to be reduced under direct sunlight.